## **RSC Advances**



## **PAPER**

View Article Online
View Journal | View Issue



Cite this: RSC Adv., 2017, 7, 3790

# Efficient conversion of fructose into 5-hydroxymethylfurfural over WO<sub>3</sub>/reduced graphene oxide catalysts†

Huatao Han, Hongyan Zhao, Yang Liu, Zhuofei Li, Jinyi Song, Wenyi Chu\* and Zhizhong Sun\*

A sustainable and efficient catalyst for converting carbohydrates to a renewable platform chemical 5-hydroxymethylfurfural (HMF) is the goal in the study of biomass recycling. Reduced graphene oxide-supported tungsten trioxide (WO<sub>3</sub>/RGO) as an acidic catalyst was synthesized through a one-step hydrothermal method, characterized *via* TEM, XPS, XRD and Raman spectroscopy and applied to the conversion of fructose to HMF. The WO<sub>3</sub>/RGO catalyst showed a highly efficient catalytic activity, and the yield of HMF could reach up to 84.2% with complete conversion of fructose. The catalyst could be reused five times with a slight decrease in activity. Further study indicated that WO<sub>3</sub>/RGO could also catalyze the conversion of cellulose, glucose and sucrose to HMF.

Received 4th November 2016 Accepted 16th December 2016

DOI: 10.1039/c6ra26309g

www.rsc.org/advances

#### Introduction

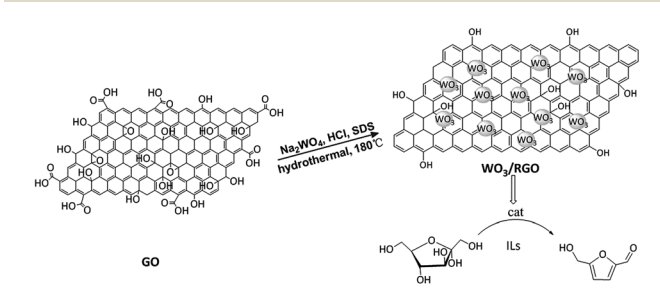
The burning of fossil fuels does great harm to the ecological environment, and the depletion of non-renewable energy makes humans face a great challenge. Biomass as the sole renewable carbon source can guarantee the sustainable use of energy.<sup>1,2</sup> Therefore, the conversion of biomass into fuels, chemicals and materials has received broad attention.<sup>3-6</sup> 5-Hydroxymethylfurfural (HMF), produced from the acid-catalyzed dehydration of hexose, is an important platform chemical between carbohydrate biomass and the oil industry.<sup>7-10</sup>

Although formation of HMF from abundant renewable carbohydrates, such as glucose and fructose, has been achieved, scientists are still aiming to research and develop a type of green and efficient catalyst. A series of acid catalysts, such as various mineral acids, 11,12 metal Lewis acids, 13-15 organic acids, 16 and acidic ionic liquids, 7,17 were synthesized and used in HMF production from fructose, glucose and other sugars. Supported transition metal oxide composites, the same as solid acid catalysts used in HMF formation, form sugars due to their Brønsted or Lewis acid sites. 18-20 For several acid-catalyzed conversions of biomass, the acidity of the supported transition metal oxide plays a crucial role in the reaction. Nevertheless, the structural instability under severe conditions and lower dispersability of a traditional solvent in a carrier material remains a concern.

School of Chemistry and Materials Science, Heilongjiang University, Harbin 150080, P. R. China. E-mail: wenyichu@hlju.edu.cn; sunzz@hlju.edu.cn

Graphene, as one of the most promising carbon nanomaterials, provides a template to anchor active species for catalysis due to its unique two-dimensional structure, strong surface area, and superior mechanical and electrical transmission performance.21-23 Therefore, graphene-based materials have become the focal points in the growing field of carbocatalysis in recent years.24-26 Our previous study proved that Pd@PdO-NDG27 and Cu NPs@RGO28 could act as an effective catalyst in organic reactions. In addition, tungsten oxide (WO<sub>3</sub>), as an acidic catalyst, had been used for biomass conversion. Prasenjit Bhaumik et al.29 reported silica-supported WO<sub>3</sub> as a solid acid catalyst in the synthesis of furfural, directly from lignocellulosic biomass. Yue Liu et al.30 reported that WO3 catalyzed the conversion of cellulose into propylene glycol and ethylene glycol. Therefore, WO<sub>3</sub>/RGO, which was prepared by tungsten trioxide loaded onto the surface of reduced graphene oxide, could be used as an acidic catalyst with considerable value and research prospects for conversion of biomass.

In Scheme 1, reduced graphene oxide-supported tungsten trioxide (WO<sub>3</sub>/RGO) was designed and synthesized through



Scheme 1 The synthesis and application of WO<sub>3</sub>/RGO.

<sup>†</sup> Electronic supplementary information (ESI) available. See DOI: 10.1039/c6ra26309g

**RSC Advances** Paper

a simple one-step hydrothermal method. WO<sub>3</sub>/RGO, as an acid catalyst, was studied for conversion of sugars to HMF due to its acid-catalytic performance. A high HMF yield (up to 84.2%) was obtained using WO<sub>3</sub>/RGO catalyst in ionic liquids.

### **Experimental**

#### Synthesis of WO<sub>3</sub>/RGO composites

Graphene oxide (GO) was synthesized by the modified Hummer's<sup>31</sup> method. Exfoliate graphite, as the starting material, was oxidized by potassium permanganate and concentrated sulfuric acid. WO<sub>3</sub>/RGO composites were synthesized through a one-step hydrothermal method. GO was dispersed into deionized water and then sonicated for 0.5 hours to create a homogeneous dispersion (1 mg mL<sup>-1</sup>). Then, 0.3 g Na<sub>2</sub>WO<sub>4</sub>-·2H<sub>2</sub>O, 0.05 g sodium dodecyl sulfate (SDS) and 0.05 g NaCl were dissolved in 20 mL GO dispersion and kept stirring for 1 hour. The pH of the dispersion was adjusted to about 1.5 using HCl solution. After stirring for 3 hours, the suspension was transferred to a 25 mL Teflon-lined stainless steel autoclave and heated to 180 °C. The suspension was maintained for 24 hours and naturally cooled to room temperature. The final product was washed with deionized water and ethanol, dried at 50 °C for 12 hours and heated at 350 °C in a muffle furnace under nitrogen atmosphere for 6 hours with a heating rate of 15 °C min<sup>-1</sup> under nitrogen atmosphere. The catalyst was obtained with an 8.7% RGO mass content in the WO<sub>3</sub>/RGO.

Changing the amount of GO resulted in 4.5% and 12.5% of RGO obtained in the WO<sub>3</sub>/RGO. Pure WO<sub>3</sub> was obtained under the same condition without adding GO in the process.

#### Catalytic reaction procedure

In a typical experiment for the synthesis of HMF from fructose, 1 mmol fructose was added in 2.0 g of 1-butyl-3methylimidazolium chloride ([BMIM]Cl) in a small reaction vessel, and 10 mg catalyst of WO<sub>3</sub>/RGO was subsequently added. The reaction mixture was stirred and kept 120 °C. After the reaction, the mixture was transferred into 5 mL distilled water. The catalyst was separated via filtration and recycled; the filtrate was extracted with ethyl acetate (5 mL  $\times$  3). The organic phase was collected, dried with anhydrous sodium sulphate, and the solvent was evaporated by rotary evaporator to obtain pure HMF. The production and aqueous phase were analyzed via high-pressure liquid chromatography (HPLC).9,10 The yield of HMF and fructose conversion rate were calculated from a calibration curve.

HMF was identified via <sup>1</sup>H NMR spectroscopy. <sup>1</sup>H NMR (400 MHz, CDCl<sub>3</sub>):  $\delta_{\rm H}$  (400 MHz, CDCl<sub>3</sub>) 9.56 (1H, s), 7.23 (1H, d, J 3.5), 6.52 (1H, d, J 3.5), 4.71 (2H, s).

#### Results and discussion

#### Characterization of WO<sub>3</sub>/RGO catalyst

The morphology and microstructure of the obtained WO<sub>3</sub>/RGO were characterized via transmission electron microscopy (TEM) and are shown in Fig. 1. Fig. 1(a) shows the TEM image of RGO

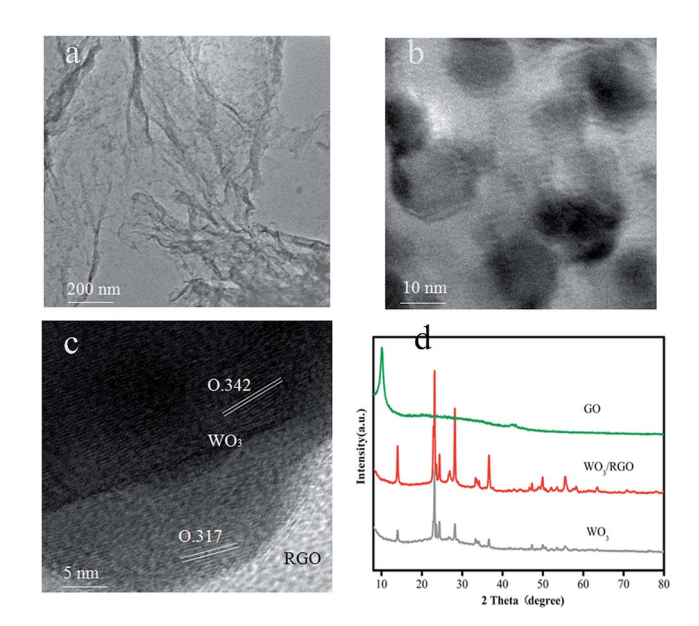


Fig. 1 TEM images of (a) RGO and (b) WO<sub>3</sub>/RGO, (c) HRTEM images of WO<sub>3</sub>/RGO, (d) XRD patterns of the GO, WO<sub>3</sub>/RGO and pure WO<sub>3</sub> samples.

to be a 2D sheet structure with crinkles. As shown in Fig. 1(b), the WO<sub>3</sub> nanoparticles, dispersed on graphene, had a 12-15 nm average diameter. The HRTEM image in Fig. 1(c) revealed lattice fringes with a 0.342 and 0.314 nm uniform interlayer distance corresponding to the (001) and (200) WO<sub>3</sub> lattice planes.

X-ray diffraction (XRD) was used to characterize the sample structure. The XRD of GO, WO<sub>3</sub>/RGO and pure WO<sub>3</sub> are shown in Fig. 1(d). The diffraction peaks of WO<sub>3</sub>/RGO and pure WO<sub>3</sub> correspond well to a standard XRD spectrum (JCPDS: 33-1387), which proved their excellent crystalline form. The disappearance of the strong diffraction peak around 10.2° of graphene oxide in the diffraction peak of WO<sub>3</sub>/RGO proved that graphene oxide was reduced to graphene. There is no evident diffraction peak of graphene in the WO<sub>3</sub>/RGO diffraction pattern because the weak graphene diffraction peaks may be masked by the WO<sub>3</sub> peak.

The FTIR spectra of WO<sub>3</sub> and WO<sub>3</sub>/RGO catalyst are shown in Fig. 2(a). The prominent broad and strong absorption band at a high frequency of 3428 cm<sup>-1</sup> is ascribed to the O-H stretching vibration. The characteristic absorption bands of GO were observed at 1047 cm<sup>-1</sup> (C-OH), 1634 cm<sup>-1</sup> (C=C) and 1733 cm<sup>-1</sup> (C=O). The broad absorption band of the WO<sub>3</sub>/RGO composite at low frequencies is ascribed to the W-O-W bond vibration. Moreover, as demonstrated in the WO<sub>3</sub>/RGO FTIR spectrum, the GO peaks corresponding to C=O and C-OH vibrations at 1733 cm<sup>-1</sup> and 1047 cm<sup>-1</sup> were not observed. The absorption band at 1610 cm<sup>-1</sup> might be attributed to the skeletal vibration of the RGO sheets. These results indicated that the original GO was reduced to RGO in the process of preparing WO<sub>3</sub>/RGO.

The Raman spectra of WO<sub>3</sub>, GO and WO<sub>3</sub>/RGO are shown in Fig. 2(b). The D and G peaks of GO and WO<sub>3</sub>/RGO appear at 1352 cm<sup>-1</sup> and 1573 cm<sup>-1</sup>. In the Raman spectrum of WO<sub>3</sub>/ RGO, sharp peaks belonging to WO<sub>3</sub> could be observed. Raman



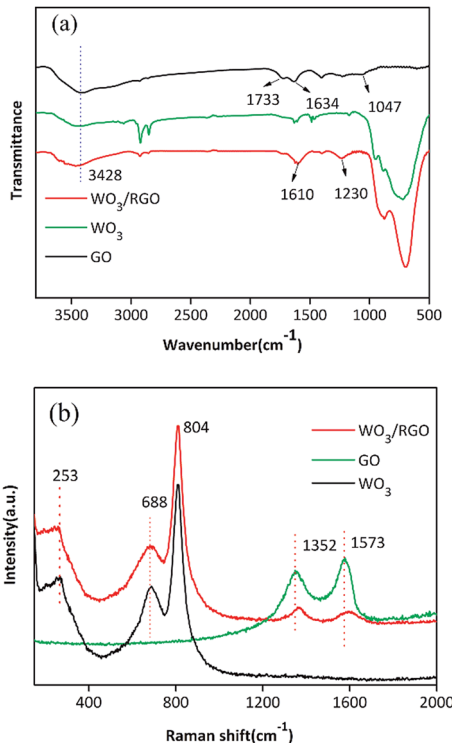


Fig. 2 (a) FT-IR spectra of WO $_3$ , GO and WO $_3$ /RGO. (b) Raman spectra of WO $_3$ , GO and WO $_3$ /RGO.

bands of 804 cm<sup>-1</sup> and 688 cm<sup>-1</sup> correspond to the O-W-O stretching modes, which are the main characteristic peaks of WO<sub>3</sub> crystallites. The band located at 253 cm<sup>-1</sup> is related to the W-O-W bending mode for WO<sub>3</sub>. Compared with that of pure WO<sub>3</sub>, the peak at 688 cm<sup>-1</sup> was slightly lower, probably due to the formation of C-O-W bonds between the graphene and WO<sub>3</sub> nanoparticles.<sup>32</sup> This chemical bond indicated that WO<sub>3</sub> was chemically bonded to the surface of graphene layer *via* C-O-W bonds rather than physically interacting with graphene.

X-ray photoelectron spectroscopy (XPS) was used to investigate the surface element composition of catalysts and the corresponding valence state. As shown in Fig. 3(a), the C 1s XPS spectrum of GO was defined by four peaks, corresponding to C atoms in several representative functional groups of C-C (284.6 eV), C-O (hydroxyl and epoxy groups, 286.6 eV), C=O (287.7 eV) and the carbonyl C at 288.9 eV. Fig. 3(b) shows the full spectrum of WO<sub>3</sub>/RGO catalyst. It could be clearly observed that the sample consisted of W, O, and C elements without impurities. The peaks of W 4f, O 1s, C 1s were very close to the XPS results provided by the literature reported for WO<sub>3</sub>.33 According to the C 1s XPS spectrum of WO<sub>3</sub>/RGO in Fig. 3(c), the carbonyl C at 288.9 eV had disappeared, the C=O (288 eV) and the C-O (286.1 eV) signal decreased markedly in intensity compared with C 1s of GO. It proved that GO had been reduced to graphene accompanied by elimination of the oxygen-containing group. The spectrum W 4f of WO<sub>3</sub>/RGO in Fig. 3(d) shows two peaks at 35.1 eV and 38.2 eV that could be ascribed to W  $4f_{7/2}$  and W  $4f_{5/2}$ , respectively. These results completely correspond to the valence of W<sup>6+</sup>. However, the binding energy value of W 4f<sub>7/2</sub> located at

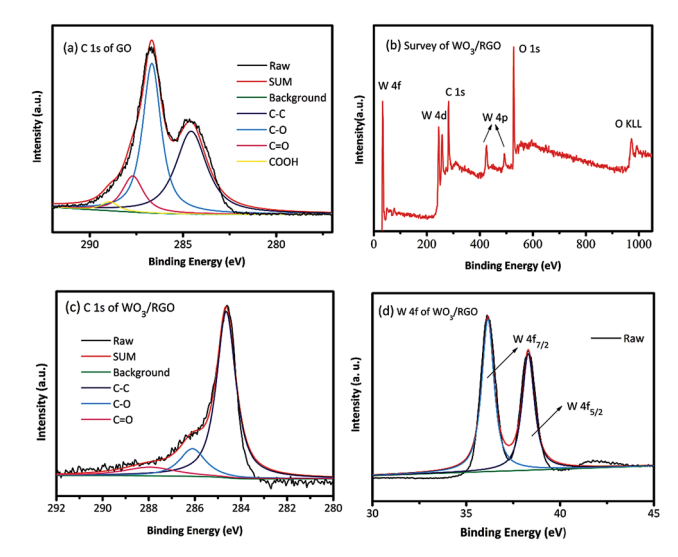
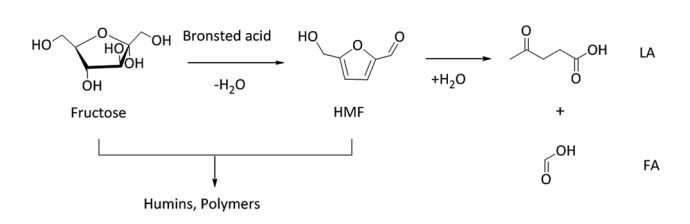


Fig. 3 (a) C 1s XPS of GO, (b) the full spectra of WO $_3$ /RGO, (c) C 1s of WO $_3$ /RGO, (d) W 4f of WO $_3$ /RGO.

35.1 eV was slightly lower than that of pure WO<sub>3</sub>;<sup>33,34</sup> such a shift might be attributed to the interaction between WO<sub>3</sub> and graphene (Scheme 2).

#### Catalytic reactions

To evaluate the catalytic performance of WO<sub>3</sub>/RGO, various catalysts were used under identical reaction conditions, and the results are summarized in Table 1. Fructose was converted to HMF in experimental conditions including 1 mmol fructose, 10 mg catalyst, 2.0 g [BMIM]Cl and 2 hours reaction time. According to comparison (Table 1, entries 1-3), 8.7% RGO content in the catalyst obtained the highest fructose conversion (100%) and HMF yield (82.9%). Humins and polymers were be formed during the reaction, and the generated HMF was further hydrolyzed to levulinic acid (LA) and formic acid (FA),9,10 which would lead to a decrease in the HMF selectivity (Scheme 1). HMF was hydrolysed into equimolar amounts of LA and FA. The yield of FA was lower than LA due to the decomposition of FA during the reaction.6 The reaction without catalyst gave a much lower HMF yield (Table 1, entry 4). The yield of HMF with GO as the catalyst was 67.4% (Table 1, entry 5). GO possessed catalytic activity because it contains large amounts of carboxylic acid functional groups. When used WO3 with no carrier materials, the HMF yield was 62.5% (Table 1, entry 6). WO<sub>3</sub>/RGO exhibited excellent catalytic performance because the presence of RGO can increase the contact area between the catalyst and the



Scheme 2 Fructose conversion into HMF and its by-products.

8.7

4.9

Cellulose<sup>d</sup>

14

Entry	Substrate	Catalyst	T (°C)	Conversion $^b$ (%)	Yield <sup>b</sup> (%)		
					HMF <sup>[Ref]</sup>	LA	FA
1	Fructose	WO <sub>3</sub> /RGO (4.5%)	120	87.2	67.8	2.1	0.8
2	Fructose	WO <sub>3</sub> /RGO (8.7%)	120	100	84.2	5.2	3.1
3	Fructose	WO <sub>3</sub> /RGO (12.5%)	120	94.2	74.3	3.8	1.6
4	Fructose	_ ` ` ` `	120	57.0	22.6	0.5	<0.1
5	Fructose	GO	120	86.6	67.4	3.4	1.3
6	Fructose	$WO_3$	120	88.0	62.5	1.9	0.6
7	Fructose	$H_2SO_4$	120	69.2	41.8	9.4	5.2
8	Fructose	$H_3PW_{12}O_{40}$	80	100	$99.0^{[12]}$	_	
9	Fructose	$WO_3/ZrO_2$	120	100	$94.0^{[14]}$	2	
10	Fructose	SBA-15	140	89.2	$41.9^{[18]}$	_	_
11	Fructose	ZSM-5	170	89.0	$75.0^{[11]}$	_	_
12	Glucose	WO <sub>3</sub> /RGO	140	58.6	36.4	0.8	< 0.1
13	Sucrose <sup>c</sup>	WO <sub>3</sub> /RGO	140	70.2	51.2	1.1	<0.1

Table 1 Catalytic performance of fructose to HMF over different catalysts<sup>a</sup>

WO<sub>3</sub>/RGO

44.6

180

substrate. Moreover, large amounts of hydroxyl groups on the surface of RGO promoted the catalyst dispersion in the solvent. H<sub>3</sub>PW<sub>12</sub>O<sub>40</sub> and H<sub>2</sub>SO<sub>4</sub>, with strong Brønsted acid sites, could participate in homogeneous catalysis. With H<sub>2</sub>SO<sub>4</sub> as the catalyst, a lower yield of HMF (41.8%) was obtained with more formation of LA (9.4%) and FA (5.2%) (Table 1, entry 7). With H<sub>3</sub>PW<sub>12</sub>O<sub>40</sub> as the catalyst, a relatively higher HMF yield of up to 99.0% was obtained (Table 1, entry 8). Unfortunately, it brought great trouble in the separation of production and recycling of catalyst. Compared with WO<sub>3</sub>/RGO, WO<sub>3</sub>/ZrO<sub>2</sub> as a catalyst gave a higher HMP yield (94.0%) (Table 1, entry 9). With SBA-15 and ZSM-5, the typical solid-acid catalysts, the yields of HMF were 41.9% and 75.0%, respectively (Table 1, entries 10 and 11). Glucose, sucrose and cellulose could also be converted to HMF (Table 1, entries 12-14) and the yields were 36.4%, 51.2% and 18.8%, respectively. With cellulose as a substrate, increasing the temperature increased the cellulose conversion, but the selectivity of HMF decreased greatly. Cellulose conversions were determined by measuring the difference in the weight of cellulose before and after the reaction.30 The molar quantities of cellulose were calculated based on the molecular weight of the C<sub>6</sub>H<sub>10</sub>O<sub>5</sub> unit.

The abovementioned results unequivocally demonstrated that WO<sub>3</sub>/RGO was an outstanding acidic catalyst. In order to further investigate the influence of the catalyst in the reaction, WO<sub>3</sub>/RGO was used as a catalyst to optimize the reaction conditions including catalyst weight, solvents and temperature. First, different loadings of catalyst including 20 mg, 15 mg, 10 mg and 5 mg were screened (Fig. 4(a)). The use of 5 mg WO<sub>3</sub>/RGO catalyst obtained HMF in only 44.3% yield with 72.5% fructose conversion. The catalyst loading was 10 mg to give the highest yield of HMF up to 84.2% with complete conversion of fructose. The yields would reduce slightly with increased catalyst weight. The solvent, as an important influential factor for the catalytic reaction, was also screened.

As shown in the Fig. 4(b), it was clear that the highest yield of the reaction that could be achieved was 84.2% with a complete conversion rate of fructose in [BMIM]Cl. In water, the obtained yield of HMF (16.4%) was low, whereas the fructose conversion (38.2%) and the yield of LA was much higher than others. Only 21% and 38% HMF yields could be obtained using [BMIM]Tf<sub>2</sub>N, [BMIM]BF<sub>4</sub> as solvents, respectively. As is known, DMSO is a common solvent that could be used in

18.8

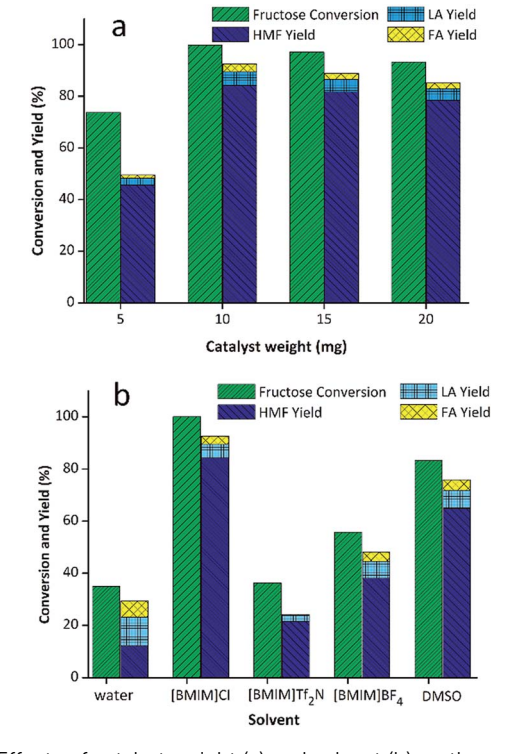


Fig. 4 Effects of catalyst weight (a) and solvent (b) on the conversion of fructose to HMF.

<sup>&</sup>lt;sup>a</sup> Reaction conditions: substrate (1 mmol), catalyst 10 mg, [BMIM]Cl 2.0 g, 2 hours. <sup>b</sup> Determined by HPLC analysis. <sup>c</sup> Sucrose 0.5 mmol, catalyst 10 mg, [BMIM]Cl 2.0 g, 2 hours. <sup>d</sup> Cellulose 1.5 g, catalyst 100 mg, [BMIM]Cl/ $H_2O$  1 : 4 (10 mL), closed system 8 hours, the conversion (wt%) was calculated by the weight of cellulose before and after reaction.

RSC Advances Paper

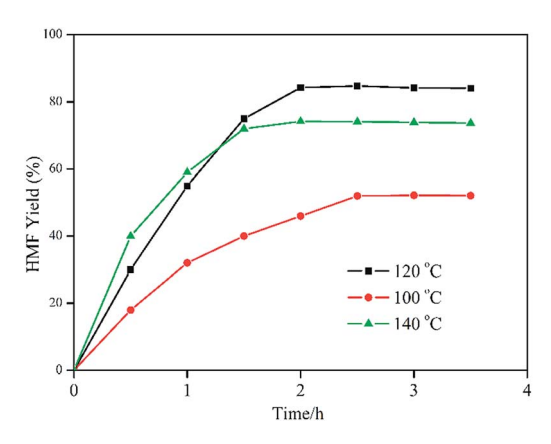


Fig. 5 Effects of reaction temperature and reaction time on the conversion of fructose to HMF.

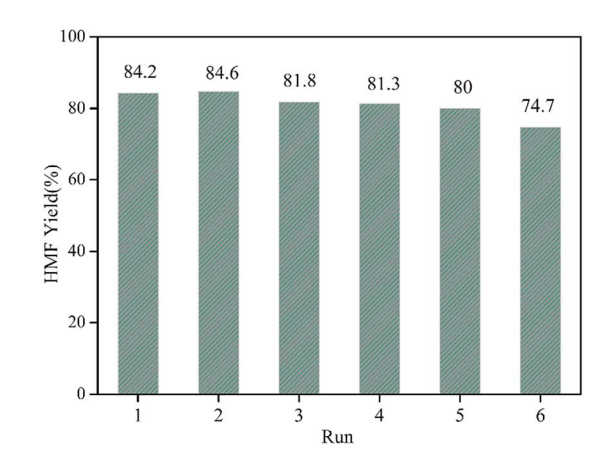


Fig. 6 Recycling of the WO<sub>3</sub>/RGO catalyst.

HMF production, but with this solvent only a 64.8% yield was obtained.

Fig. 5 exhibits the effects of reaction temperature and reaction time on the fructose to HMF conversion. Following the reaction progresses, HMF was constantly generated. When the reaction was performed at 100 °C, the rate of HMF formation was rather slow. Even with a further prolonged reaction time to 2.5 hours, the yield was only 52.2%. The maximum HMF yield of 84.2% with a full fructose conversion was obtained at 120 °C after a 2 hour reaction time. When the reaction temperature was raised to 140 °C, the reaction rate increased. While the yield of HMF decreased to 74.1% because of the further hydrolysis of HMF at an excessively high temperature.

Apart from efficient catalytic activity, the recoverability and stability are significant criteria for solid catalysts. In order to attest the reusability of  $WO_3/RGO$  catalyst, a six-cycle experiment was performed, and the results are shown in Fig. 6. The catalyst retained considerable activity after five cycles. Five reuse cycles showed that the yield of HMF was always over 80%, although it gradually decreased. The yield of HMF at the sixth cycle decreased to 74.7% due to the depressed activity of catalyst with frequent use.

#### Conclusions

In conclusion, the reduced graphene oxide supported tungsten trioxide (WO<sub>3</sub>/RGO) was prepared via a one-step hydrothermal method and used as an active acid catalyst for fructose to HMF conversion. A high yield of HMF up to 84.2% with a full fructose conversion was obtained with the catalyst under the optimum reaction conditions: 1 mmol fructose, 10 mg WO<sub>3</sub>/RGO, 2.0 g [BMIM]Cl, 120 °C for 2 hours. Moreover, it could also transform cellulose, glucose and sucrose to HMF despite having a relatively lower yield. WO<sub>3</sub>/RGO was proven to be a more suitable catalyst for fructose conversion. The catalyst could be reused five times with a slight decrease in activity.

## Acknowledgements

The authors thank the financial support from the Research Project of the Natural Science Foundation of Heilongjiang Province of China (No. B201207 and No. B201208).

#### Notes and references

- 1 Y. Chisti, Biotechnol. Adv., 2007, 25, 294-306.
- 2 J. J. Bozell, Science, 2010, 329, 522-523.
- 3 A. Corma, S. Iborra and A. Velty, *Chem. Rev.*, 2007, **107**, 2411–2502.
- 4 R. Rinaldi and F. Schüth, *Energy Environ. Sci.*, 2009, **2**, 610–626.
- 5 D. Ding, J. Wang, J. Xi, X. Liu, G. Lu and Y. Wang, Green Chem., 2014, 16, 3846–3853.
- 6 P. P. Upare, J.-W. Yoon, M. Y. Kim, H.-Y. Kong, D. W. Hwang, Y. K. Hwang, H. H. Kung and J.-S. Chang, *Green Chem.*, 2013, 15, 2935–2943.
- 7 H. Zhao, J. E. Holladay, H. Brown and Z. C. Zhang, Science, 2007, 316, 1597–1600.
- 8 R. J. van Putten, J. C. van der Waal, E. de Jong, C. B. Rasrendra, H. J. Heeres and J. G. de Vries, *Chem. Rev.*, 2013, 113, 1499–1597.
- 9 Y. Jiang, L. Yang, C. M. Bohn, G. Li, D. Han, N. S. Mosier, J. T. Miller, H. I. Kenttämaa and M. M. Abu-Omar, *Org. Chem. Front.*, 2015, **2**, 1388–1396.
- 10 A. Ranoux, K. Djanashvili, I. W. C. E. Arends and U. Hanefeld, ACS Catal., 2013, 3, 760–763.
- 11 D. W. Gardner, J. Huo, T. C. Hoff, R. L. Johnson, B. H. Shanks and J.-P. Tessonnier, ACS Catal., 2015, 5, 4418–4422.
- 12 Y. Xiao and Y.-F. Song, Appl. Catal., A, 2014, 484, 74-78.
- 13 A. Chinnappan, A. H. Jadhav, W.-J. Chung and H. Kim, *Ind. Crops Prod.*, 2015, **76**, 12–17.
- 14 K. Shimizu, R. Uozumi and A. Satsuma, *Catal. Commun.*, 2009, **10**, 1849–1853.
- 15 J. B. Binder, A. V. Cefali, J. J. Blank and R. T. Raines, *Energy Environ. Sci.*, 2010, 3, 765–771.
- 16 S. Hu, Z. Zhang, Y. Zhou, J. Song, H. Fan and B. Han, *Green Chem.*, 2009, 11, 873–877.
- 17 D. D. J. Liu and E. Y.-X. Chen, *Appl. Catal.*, *A*, 2012, 435–436, 78–85.

Paper

- 18 X. Guo, Q. Cao, Y. Jiang, J. Guan, X. Wang and X. Mu, Carbohydr. Res., 2012, 351, 35-41.
- 19 B. Liu and Z. Zhang, ACS Catal., 2016, 6, 326-338.
- 20 A. Chareonlimkun, V. Champreda, A. Shotipruk and N. Laosiripojana, *Bioresour. Technol.*, 2010, **101**, 4179–4186.
- 21 P. Goli, H. Ning, X. Li, C. Y. Lu, K. S. Novoselov and A. A. Balandin, Nano Lett., 2014, 14, 1497-1503.
- 22 Q. Huang, L. Zhou, X. Jiang, Y. Zhou, H. Fan and W. Lang, ACS Appl. Mater. Interfaces, 2014, 6, 13502-13509.
- 23 B. F. Machado and P. Serp, Catal. Sci. Technol., 2012, 2, 54-75.
- 24 S. Navalon, A. Dhakshinamoorthy, M. Alvaro and H. Garcia, Chem. Rev., 2014, 114, 6179-6212.
- 25 H. Huang, Z. Yue, G. Li, X. Wang, J. Huang, Y. Du and P. Yang, J. Mater. Chem. A, 2013, 1, 15110-15116.
- 26 L. Wang, X. Lu, S. Lei and Y. Song, J. Mater. Chem. A, 2014, 2, 4491-4509.

- 27 B. Jiang, S. Song, J. Wang, Y. Xie, W. Chu, H. Li, H. Xu, C. Tian and H. Fu, Nano Res., 2014, 7, 1280-1290.
- 28 H. Zhao, G. Mao, H. Han, J. Song, Y. Liu, W. Chu and Z. Sun, RSC Adv., 2016, 6, 41108-41113.
- 29 P. Bhaumik and P. L. Dhepe, ChemCatChem, 2016, 8, 1-9.
- 30 Y. Liu, C. Luo and H. Liu, Angew. Chem., Int. Ed., 2012, 51, 3249-3253.
- 31 D. C. Marcano, D. V. Kosynkin, J. M. Berlin, A. Sinitskii, Z. Z. Sun, A. Slesarev, L. B. Alemany, W. Lu and J. M. Tour, ACS Nano, 2010, 4, 4806-4814.
- 32 J. Guo, Y. Li, S. Zhu, Z. Chen, Q. Liu, D. Zhang, W.-J. Moon and D.-M. Song, RSC Adv., 2012, 2, 1356-1363.
- 33 B. Weng, J. Wu, N. Zhang and Y.-J. Xu, Langmuir, 2014, 30, 5574-5584.
- 34 L. Huang, H. Xu, Y. Li, H. Li, X. Cheng, J. Xia, Y. Xu and G. Cai, Dalton Trans., 2013, 42, 8606-8616.